Top Organomet Chem
DOI: 10.1007/3418_2016_4

Sulfur-Supported Iron Complexes for Understanding N_2 Reduction

Amy L. Speelman and Patrick L. Holland

Abstract This chapter focuses on the use of synthetic complexes for modeling iron sites in the iron-molybdenum nitrogenase enzyme, particularly on those with sulfur donors in the coordination sphere. This is an under-explored area that has promise to elucidate the way that Fe–S bonds contribute to N_2 binding and activation. We review iron complexes with sulfide, thiolate, and thioether-containing supporting ligands and discuss the binding of N_2 as well as reduced species such as hydrazine and diazene. The structures, spectroscopy, reactions, and other properties of key complexes are described, including recent results.

Keywords Dinitrogen • Iron • Nitrogenase • Sulfur

Contents

1 N_2 Reduction in Biological Systems
2 Fe–N_2 Complexes with S Ligands
  2.1 N_2 Complexes with Thioether-Containing Ligands
  2.2 N_2 Complexes with Thiolate Ligands
  2.3 Interaction of N_2 with Iron–Sulfide Clusters
3 Fe Complexes with N_xH_y Ligands
  3.1 N_xH_y Complexes with Iron–Sulfide Clusters
  3.2 N_xH_y Complexes with Thioether/Thiolate Ligands
  3.3 N_xH_y Complexes with Thiolate Ligands
  3.4 N_xH_y Complexes with Thiolate and Cp Ligands
4 Conclusions
References

A.L. Speelman and P.L. Holland (✉)
Department of Chemistry, Yale University, New Haven, CT 06520, USA
e-mail: patrick.holland@yale.edu

1 N_2 Reduction in Biological Systems

Nitrogen atoms are essential building blocks of biomacromolecules. Although atmospheric dinitrogen is a plentiful source of N atoms, N_2 is relatively inert and only specialized organisms are capable of "fixing" N_2 to a bioavailable form such as ammonia or nitrate [1]. In these nitrogen-processing ("diazotrophic") bacteria and archaea, biological nitrogen fixation is catalyzed by nitrogenase enzymes according to the overall idealized reaction stoichiometry [2]:

$$N_2 + 8\,H^+ + 8\,e^- + 16\,ATP \rightarrow 2\,NH_3 + H_2 + 16\,ADP + 16\,phosphate$$

Nitrogenase enzymes are complicated multicomponent systems, and the reader may look elsewhere for detailed descriptions of their enzymology [3–5]. Here, we focus on the inorganic chemistry at the N_2-binding cofactors, which are metalloclusters called the FeMoco (in molybdenum-dependent nitrogenases), the FeVco (in vanadium-dependent nitrogenases), or the FeFeco (in iron-only nitrogenases). Thus far, the only structurally characterized one of these cofactors is the FeMoco, which is an unusual [Fe_7MoS_9C] cluster (Fig. 1). In alternative nitrogenases, the molybdenum center is replaced by vanadium or iron, but the overall shape of the cofactor is thought to be similar [6, 7]. Based on the shared reactivity of all nitrogenase variants, as well as mutagenesis studies that show loss of N_2 reduction ability upon mutation of His^{195} and Val^{70} (Fig. 1; numbering is for *Azotobacter vinelandii* FeMo-nitrogenase), the central iron atoms are most strongly implicated as the site of N_2 binding [8].

Given the importance of nitrogenases in the global nitrogen cycle, and the prospect of unusual chemistry at the FeMoco, the mechanism of nitrogen reduction in the molybdenum-dependent nitrogenases has been a topic of great interest in the bioinorganic chemistry community. Substantial recent advances on the mechanism of N_2 reduction by the FeMoco come from pulsed EPR studies on trapped intermediates from Seefeldt, Hoffman, Dean, and coworkers [5, 11–14]. They have constructed models

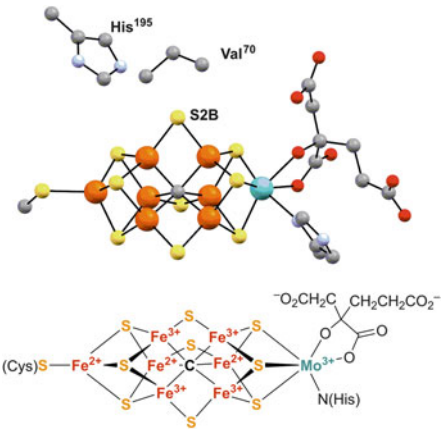

Fig. 1 Structure of the resting state of the FeMoco. (*Top*) Crystal structure of the FeMoco (PDB ID 4TKU) shown with key residues near the active site. (*Bottom*) The proposed oxidation state assignments for the iron and molybdenum ions based on spatially resolved anomalous dispersion refinement [9] and Mo K-edge X-ray absorption spectroscopy [10], respectively

that are based on the Lowe–Thorneley kinetic scheme [2, 15], which specifies that from the resting state (E_0), four electrons and four protons are added to give the intermediate E_4, which is the state that binds N_2. Electron-nuclear double resonance (ENDOR) studies indicate that E_4 has two hydrides bridging between iron centers, implying that the other two H atoms are probably protonated sulfides [16–18]. According to the Lowe–Thorneley model, the reversible reductive elimination of H_2 is accompanied by N_2 binding to iron [15]. Seefeldt and Hoffman propose that the bound N_2 is immediately converted to a species at the diazene redox level, although the steps in this transformation and the structure of the resulting "N_2H_2" species are not clear. The sites of subsequent protonation are also unclear, but the possibilities are typically categorized as distal and alternating (see Fig. 2). In the distal pathway, proposed by analogy to small molecule molybdenum complexes [19, 20], the first molecule of ammonia is released following three protonations at the distal nitrogen. This results in the formation of a nitride that can accept three more protons and electrons to release a second equivalent of ammonia. In the alternating pathway, each N atom is protonated in turn to eventually yield a hydrazine species that undergoes N–N bond cleavage. The alternating mechanism has generally been favored for the FeMoco on the basis that diazene and hydrazine (which are intermediates unique to the alternating pathway) are also nitrogenase substrates, and that hydrazine is released from the enzyme during turnover under some conditions [5]. Although species following N–N cleavage (which are common to both the alternating and distal pathways) have been trapped and characterized by pulsed EPR [5], no intermediate that is unique to the distal or alternating pathway has been observed in the FeMoco. Furthermore, a recent study of a model complex suggests that crossover between intermediates in the distal and alternating pathways should also be considered [21]. Within each limiting mechanism, there are additional ambiguities to be resolved because the intermediates may be terminally bound or bridging between metal centers, and their coordination modes could change throughout the catalytic cycle. Thus, many questions remain about the mechanism of NH_3 formation, even in the best-understood nitrogenase.

Only the resting state of the FeMoco has been structurally characterized. Rearrangement of synthetic iron–sulfur clusters upon ligand binding or redox changes is known [22–24], and therefore it is reasonable to predict that internal bond cleavage might occur upon reduction and N_2 binding in the FeMoco. Additional evidence for this hypothesis comes from experimental studies of nitrogenase. For example, in the crystal structure of the CO-inhibited form of nitrogenase, one of the central bridging sulfides (S2B; see Fig. 1) is replaced by CO [25]. When CO is removed and the enzyme is exposed to catalytic conditions, the bridging sulfide is reincorporated and the enzyme regains full activity. In another example, Rees and coworkers replaced S2B with a selenide. Crystallographic studies demonstrated that the selenide migrates to the other central "belt" sites and is eventually extruded from the active site (with reincorporation of a sulfide) during acetylene reduction [26]. The fate of the released S^{2-} or Se^{2-} and the mechanism of the exchange processes in these experiments are not yet clear. Nevertheless, these studies demonstrate that sulfide dissociation and cluster rearrangement certainly can occur during turnover. However, ^{13}C and ^{14}C labeling

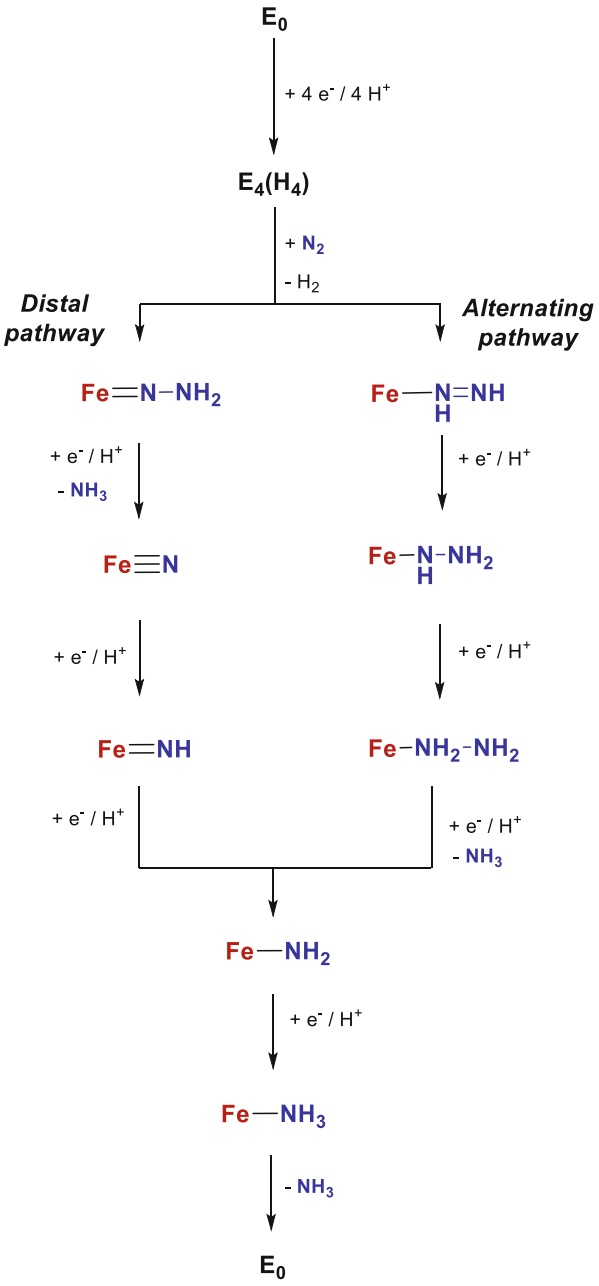

Fig. 2 Distal and alternating pathways for N_2 reduction. Although all intermediates are drawn as terminally coordinated, bridging coordination modes are also plausible

studies confirm that the central carbide does not exchange during reduction of C_2H_2, CO, or N_2 [27].

Given the uncertainty surrounding the mechanism of nitrogenase and its structure during turnover, many different intermediates could be postulated. A wide variety of mechanistic steps have been proposed based on DFT calculations [28–39]. Synthetic model compounds have been used to test the feasibility of some of these proposed chemical transformations. Iron complexes that cleave N_2 [40–43] as well as iron complexes that catalytically reduce N_2 to ammonia and/or silylamine [44–49] have been reported. However, these compounds and others that bind N_2 and/or partially reduced N_2 species (N_xH_y; $x = 1$–2, $y = 1$–4) typically contain phosphorus, nitrogen, and/or carbon donors and it is unclear what effects these abiological ligands have on catalysis. Nitrogenase-relevant compounds with these types of ligand frameworks have been reviewed elsewhere [20, 50–56].

Iron complexes with sulfur supporting ligands that bind N_xH_y fragments can give distinctive insight into the reactivity patterns that can be expected in the FeMoco [57]. As shown in the examples below, the sulfur donors may serve as functional models for sulfides, for example, by facilitating proton delivery or by stabilizing N_xH_y species through hydrogen bonding interactions. Furthermore, these complexes can replicate the weak ligand field, the low coordination number, and the high-spin electronic configuration of the iron sites in the FeMoco. Complexes containing sulfides are the most relevant to nitrogenase, but more often thiolates are used as anionic donors. A number of iron complexes with thioether ligands, which model protonated sulfides in nitrogenases, are also known. Here, we discuss these iron complexes with sulfur-containing ligands that bind N_2 and N_xH_y fragments in the context of nitrogenase modeling.

2 Fe–N_2 Complexes with S Ligands

A variety of coordination modes have been proposed for N_2 in the FeMoco [30, 33, 58]. These include bridging, terminal, and side-on coordination, in some cases involving rearrangement of the cofactor. Model complexes can illustrate the plausibility of N_2 binding in these coordination modes in a sulfur-rich coordination environment.

The interaction of N_2 with transition metals consists primarily of π-backbonding from filled iron d-orbitals into the empty π* orbitals of N_2, which results in a weakening of the N–N triple bond [50, 59]. The deviation of the N–N bond length and/or N–N stretching frequency from the values for free N_2 can be used as measures of the degree of activation of the N–N bond. The parameters for structurally characterized N_2 complexes with sulfur supporting ligands are given in Table 1. These complexes, along with other species that can be shown by reactivity or spectroscopic studies to bind N_2, are discussed below.

Table 1 Key bond lengths and N≡N stretching frequencies of N_2 complexes with sulfur donors

Complex	Fe–N (Å)	N–N (Å)	ν_{NN} (cm^{-1})	Ref.
Free N_2	–	1.098	2,359	[60]
Thioether complexes				
$[Fe(^{iPr}PDI)(N_2)]$ (**1**)	1.797(2) 1.799(2)	1.118(3) 1.111(3)	2,045	[61]
$[Fe(SiP^{iPr}{}_3)(N_2)]^+$ (**2**)	1.913(2)	1.091(3)	2,143	[62]
$[Fe(SiP^{iPr}{}_2S^{Ad})(N_2)]^+$ (**3**)	1.954(3)	1.037(5)	2,156	[63]
$[Fe(SiP^{iPr}S^{Ad}{}_2)(H)(N_2)]$ (**5**)	1.828(2)	1.116(3)	2,060	[63]
Thiolate complexes				
$[Fe^{I}(N_2)(\mu\text{-SAr})Fe^{I}(N_2)]^-$ (**7**)	1.808(1) 1.822(1)	1.128(1) 1.122(2)	2,017, 1,979	[64]
$[Fe^{I}(N_2)(\mu\text{-SAr})Fe^{II}(N_2)]$ (**8**)	1.854(7)	1.05(1)	2,070, 1,983	[64]
$[Fe^{II}(N_2)(\mu\text{-SAr})Fe^{II}(N_2)]^+$ (**9**)	1.889(3) 1.917(3)	1.048(5) 1.034(5)	2,129	[64]
$[Fe^{I}(N_2)(H)(\mu\text{-SAr})Fe^{II}(N_2)]^-$ (**10**)	1.804(3) 1.819(3)	1.124(4) 1.120(6)	1,981, 2,044	[64]
$[Fe^{II}(N_2)(H)(\mu\text{-SAr})Fe^{II}(N_2)]$ (**11**)	1.8392(9)	1.110(1)	2,036, 2,096	[64]
$[Fe(L)(N_2)]^{2-}$ (**13**)	1.790(5)	1.132(8)	1,880	[65]

Values in parentheses are estimated standard deviations (esd)

2.1 N_2 Complexes with Thioether-Containing Ligands

The first structurally characterized iron–N_2 complex with any type of sulfur donor was the tetrahydrothiophene (THT) adduct of the complex $[Fe(^{iPr}PDI)(N_2)]$ (**1**) [61] (Fig. 3). Peters and coworkers later reported a set of thioether derivatives of the complex $[Fe(SiP^{iPr})_3(N_2)]^+$ (**2**) [62, 63]. When a thioether was incorporated in place of one of the phosphine ligands in **2**, the complex was still able to bind N_2, although the replacement of the phosphine with thioether made the N_2 more labile and slightly less activated, as demonstrated by the increase in ν_{NN} from 2,143 cm^{-1} in the parent complex **2** to 2,156 cm^{-1} in **3**. When a second phosphine was replaced with a thioether, N_2 binding was no longer observed. Addition of a hydride led to N_2 binding to both the mono and bis(thioether) complexes and a more activated N_2 ligand as compared to analogous complexes without a hydride ligand, as shown by the 101 cm^{-1} decrease in ν_{NN} in **4** (ν_{NN} = 2,055 cm^{-1}) as compared to **3**. The formation of hydrides could play a similar role in promoting N_2 binding and activation in the FeMoco. Although it could not be crystallographically characterized, the mixed-valence iron(I)/iron(II) bridging N_2 complex **6** was also accessible via treatment of the solvent adduct $[Fe(SiP^{iPr}S^{Ad}{}_2)(Et_2O)]^+$ with 0.5 equivalents of $CrCp_2$ or $CoCp_2$. Complex **6** exhibits an N–N stretching vibration at 1,881 cm^{-1}, significantly lower than any of the monometallic complexes with this ligand, which illustrates how N_2 binding and activation could be facilitated by multimetallic cooperativity [66].

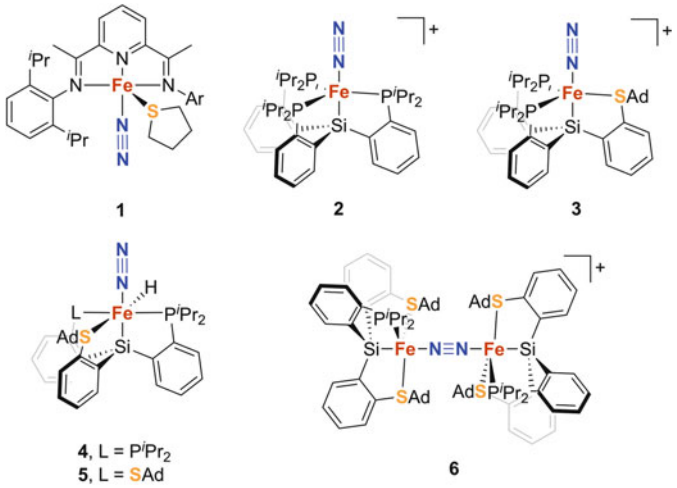

Fig. 3 N_2 complexes with thioether-containing ligands. *Ad* = adamantyl

2.2 *N_2 Complexes with Thiolate Ligands*

There are also examples of thiolate complexes with N_2 ligands. Peters and coworkers generated a series of thiolate-bridged terminal N_2 complexes in three different oxidation states (**7**–**9**) [64] (Fig. 4). Terminal hydride analogs of complexes **8** and **9** (**10** and **11**) were also reported. Complex **9** catalyzed low turnovers of NH_3 formation from N_2 but was much more effective for hydrazine disproportionation into NH_3 and N_2. Interestingly, under the same conditions the analogous monometallic complex **3** did not perform either of these reactions efficiently, suggesting that the thiolate plays an important role in catalysis, perhaps by allowing cooperativity between the iron centers and/or acting as a proton shuttle during turnover.

In complexes **3**–**11**, N_2 binding is in part promoted by the presence of phosphine ligands. More recently, it has been possible to observe N_2 binding using a supporting ligand that contains only sulfur and carbon donors [65]. Reduction of the tris(thiolate) complex **12** yielded the terminal N_2 complex **13**, in which the iron center is coordinated to two thiolates and has an η^2 interaction with the central arene ring (Fig. 5), which models a potential S_2C donor set in the FeMoco. The observation of Fe–S bond cleavage upon reduction and N_2 binding shows that dissociation of a sulfide is a chemically reasonable step for N_2 binding and activation in the FeMoco. The relatively low ν_{NN} of this complex (1,880 cm^{-1}) is indicative of an N_2 unit that is quite weakened, despite the high-spin electronic configuration of the complex. This demonstrates that a low-coordinate iron center with weak-field ligands can lead to substantial weakening of N_2 and suggests that the electron-rich thiolates lead to strong backbonding.

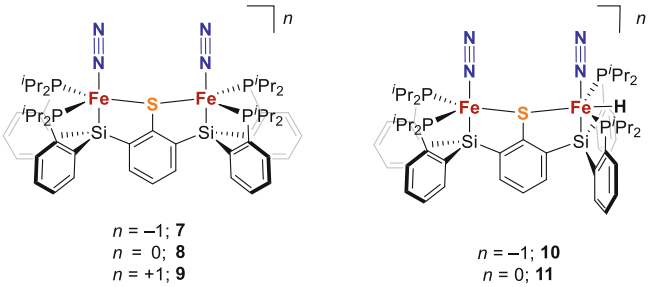

Fig. 4 N_2 complexes incorporating a bridging thiolate

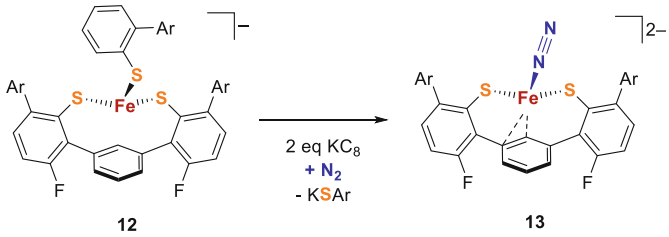

Fig. 5 N_2 binding to an iron site containing exclusively sulfur and carbon donors. *Ar* = 2,4,6-triisopropylphenyl

2.3 *Interaction of N_2 with Iron–Sulfide Clusters*

The study of synthetic iron–sulfur clusters in the context of nitrogenase has also been the topic of a significant body of work [22–24, 67, 68]. Although there are no structurally characterized iron–sulfur clusters with bound N_2 ligands, catalytic and spectroscopic studies have demonstrated that N_2 can bind to synthetic iron–sulfur clusters. Electrochemical reduction of N_2 to NH_3 is catalyzed by $[Fe_4S_4(SPh)_4]^{2-}$ and $[Mo_2Fe_6S_8(SPh)_9]^{3-}$ clusters, albeit with very low Faradaic efficiency [69]. More recently, the photochemical conversion of N_2 to NH_3 by chalcogenide aerogels (chalcogels) containing $Mo_2Fe_6S_8(SPh)_3$ and Fe_4S_4 clusters has been reported [70, 71]. Using infrared spectroscopy, N–N stretching bands were observed at 1,746 and 1,753 cm^{-1} upon irradiation of these chalcogels with visible light under N_2 atmosphere. The N–N stretching frequencies are even lower than the S_2C supported complex above and are indicative of some form of reduced N_2 species, but the redox and protonation state of this species are not known. Nevertheless, these data provide evidence for the formation of a cluster-bound N_xH_y species during turnover. N_2 binding to $Fe_2S_2^+$, $Fe_3S_3^+$, and $Fe_4S_4^+$ clusters in the gas phase has also been observed by mass spectrometry in ion-trapping experiments [72]. The structures of the N_2 adducts are not known experimentally but were suggested from DFT calculations.

Finally, in a recent study, a diferrous iron sulfide hydride complex with a β-diketiminate coligand was reduced under N_2 to give a diiron(0) N_2 complex in 24% spectroscopic yield [73]. Gas chromatography indicates that H_2 is produced during

this process. The reactivity of this complex thus models the E_4 state of the FeMoco, in which H_2 loss from an iron hydride sulfide core results in N_2 binding [14, 74–76]. However, in the model complex the H_2 production results from a bimolecular reaction, the N_2-containing product did not also contain a sulfide, and mechanistic studies of the reaction leading to sulfide extrusion and N_2 binding were precluded by the presence of a significant number of unidentified byproducts in the reaction mixture.

3 Fe Complexes with N_xH_y Ligands

There are no examples of N_2 functionalization giving a well-defined N_xH_y complex for iron complexes with sulfur supporting ligands. However, a number of diazene (HN=NH) and hydrazine (NH_2–NH_2) complexes are known with sulfur-based supporting ligands, as are alkyl- or aryl-substituted diazene and hydrazine derivatives. Generation of the hydrazine species typically proceeds in a straightforward manner by addition of hydrazine to precursor complexes. In some cases, hydrazine addition instead results in isolable diazene complexes accompanied by formation of amines, implying that the diazene was generated via hydrazine disproportionation. The generation of diazene complexes via direct addition of diazene to a precursor is more problematic because diazene is unstable in solution [77–79], but there are examples where diazene is generated and trapped in situ by iron complexes. Isolated diazene complexes are most commonly synthesized by hydrazine disproportionation or by oxidation of corresponding hydrazine species. In this section, we discuss the generation, structural characterization, and reactivity of these N_xH_y compounds.

3.1 N_xH_y Complexes with Iron–Sulfide Clusters

An early report demonstrated that the electrochemical reduction of hydrazine is catalyzed with high Faradaic efficiency by $[Fe_4S_4(SPh)_4]^{2-}$ and $[Mo_2Fe_6S_8(SPh)_9]^{3-}$ clusters, but the mechanism of NH_3 formation was not examined [80]. Chemical reduction of vanadium- and molybdenum-containing iron–sulfur cubanes also generates ammonia from hydrazine, but in all of these cases the V or Mo centers were implicated as the sites of hydrazine binding and reduction [81–89].

The only examples of structurally characterized iron N_xH_y complexes incorporating sulfides are the β-diketiminate supported complexes **14–16** [90, 91] (Fig. 6). Reaction of the diferrous monosulfide-bridged precursor with ammonia, methylhydrazine, or 1,1-dimethylhydrazine yielded 2:1 complexes in which one of the N-donors is bound to each iron center (**14**). In contrast, reaction with the parent hydrazine yielded complex **15** in which an N_2H_4 ligand bridges between the iron centers. Treatment of the diferrous precursor with 1.5 equivalents of phenylhydrazine

resulted in the formation of the mixed-valence iron(II)/iron(III) phenylhydrazido-bridged complex **16** via the overall reaction:

$$2\ \mathrm{LFe^{II}(\mu{-}S)LFe^{II}} + 3\ \mathrm{PhNH{-}NH_2} \rightarrow 2\ \mathbf{16} + \mathrm{PhNH_2} + \mathrm{NH_3}$$

This reactivity demonstrates that sulfide-bridged iron centers are capable of N–N bond cleavage. The phenylhydrazido species **16** was also the subject of a detailed ENDOR study, which enabled the first determination of the hyperfine coupling parameters of a well-defined bridging hydrazido species that could be compared to the ENDOR parameters of nitrogenase intermediates [92].

3.2 N_xH_y Complexes with Thioether/Thiolate Ligands

Sellmann and coworkers reported a series of complexes with supporting ligands containing two thiolate donors with additional thioether, amine, and/or pyridine groups [93–95]. Of particular note are several *trans* diazene complexes (two representative examples are shown in Fig. 7), which were generated either by air oxidation of a corresponding hydrazine species [96, 97] or by trapping of diazene generated in situ from potassium azodicarboxylate or benzenesulfonic acid hydrazide [98, 99]. In these complexes, the diazene ligand bridges between two iron centers, with the protons of the diazene forming one long (~2.8 Å) and one short (~2.2 Å) hydrogen bond to the

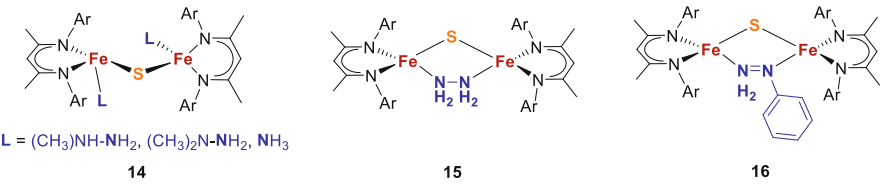

Fig. 6 Sulfide-bridged β-diketiminate complexes with nitrogenase-relevant N_xH_y fragments. *Ar* = 2,6-diisopropylphenyl

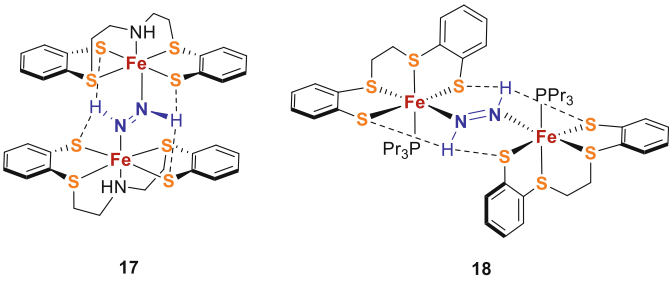

Fig. 7 Structure of diazene-bridged complexes **17** and **18**

thiolate moieties of the supporting ligand [96, 97, 99]. DFT calculations suggest that the strong hydrogen-bonding interaction contributes significantly to the overall stability of the complex [100, 101]. The sulfides in the FeMoco, as well as adjacent amino acids, may play a similar role in stabilizing intermediates during N_2 reduction. A further contribution to the stability of these complexes arises from the strong π-backbonding interaction between the iron center and the diazene ligand, as demonstrated by their intense blue color that arises from an iron to diazene charge transfer transition [102, 103]. This interaction leads to slight weakening of the N–N bond as compared to free diazene: for example, in complex **17**, the N–N bond length [96] is 1.301(5) Å compared to 1.252 Å in free diazene [104]. The N–N stretching frequency is 1,382 cm^{-1} [103], which falls between the values for free diazene ($\nu_{NN} = 1{,}529\ cm^{-1}$ [105]) and free hydrazine ($\nu_{NN} = 876\ cm^{-1}$ [106]). Using normal coordinate analysis, Lehnert and coworkers determined an N–N bond order of 1.6 for this complex indicating partial reduction to a hydrazido(2−) species [103]. SCF-Xα-SW calculations indicated that the LUMO of this complex consists primarily of a diazene π* orbital, which implies that reduction of the complex should further weaken the N–N bond of the diazene moiety [102]. However, in practice the reduction occurred at an extremely negative potential and led instead to decomposition of the complex.

Although structurally characterized monometallic iron complexes that bind hydrazine [107–109] and ammonia [107] are also known in these systems, a corresponding N_2 species could not be generated. Interestingly, however, oxidation of the diazene complex **18** with two equivalents of ferrocenium at −78 °C caused a color change from blue to purple [110, 111]. Since the HOMO of complex **18** is primarily an iron orbital [102], this oxidation was expected to result in the formation of a diferric diazene species. Warming the purple oxidized species above −40 °C resulted in N_2 evolution and formation of a green ferrous product. This implies that the purple species may be a ferrous N_2 complex, which is a valence tautomer of the expected diferric diazene complex (Fig. 8). This process would model the reverse of N_2 binding in the FeMoco and illustrate how sulfides could facilitate proton transfer. Unfortunately, the instability of the purple oxidized species prevented further characterization and its identity remains unclear.

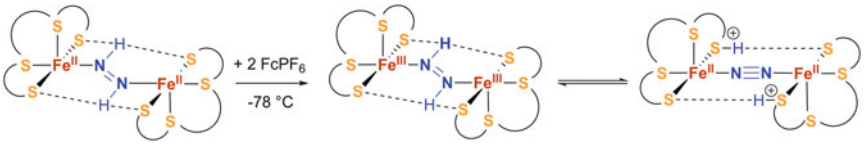

Fig. 8 Two-electron oxidation of diazene complex **18**, with the presumed product shown in two tautomeric forms: a diferric diazene complex and a diferrous dinitrogen adduct. The supporting ligands have been omitted for clarity

3.3 N_xH_y Complexes with Thiolate Ligands

Other complexes containing thiolate donors are also known to bind N_2H_4 and NH_3. In these systems, like those described above, the hydrazine ligands often form extensive hydrogen-bonding networks with the thiolates and/or solvents of crystallization. For example, Sellmann and coworkers crystallized iron bis(benzenedithiolate) complexes with hydrazine bound in bridging [112] and terminal [113] coordination modes. The terminal complex in particular contains an extensive hydrogen-bonding network between the metal-bound hydrazine and N_2H_4 and N_2H_5 molecules in the crystal lattice.

Upon reaction of the sterically hindered thiolate-bridged dimer $Fe_2(\mu\text{-STriph})_2(STriph)_2$ (STriph = 2,4,6-triphenylbenzenethiolate) with hydrazine, rearrangement to the hydrazine-bridged dimer $Fe_2(\mu\text{-}N_2H_2)_2(N_2H_2)_2(STriph)_4$ (**19**) was observed [114] (Fig. 9). The precursor complex $Fe_2(\mu\text{-STriph})_2(STriph)_2$ also reacted with amines to yield mono- and bimetallic coordination compounds and was observed to catalyze the disproportionation of 1,2-diphenylhydrazine to aniline and azobenzene (PhN=NPh). Complex **20** also coordinates ammonia and hydrazine [115]. The NH_3 and N_2H_4 ligands in **20** are labile in solution but are stabilized in the solid state by hydrogen-bonding interactions to solvent molecules. This complex catalyzes hydrazine reduction, but the number of turnovers is low and no intermediates could be observed during the reaction.

Hydrazine cleavage at iron sites has also been observed in other systems. A series of ferric iron-imide heterocubanes (**21**) were generated by the reaction of ferrous complexes containing sterically hindered thiolate ligands with 1,2-diarylhydrazines [116, 117]. The mechanism of the N–N bond cleavage step leading to imide formation is not clear but was proposed to occur through formation of a diferrous complex containing an arylhydrazine bound in a $\mu\text{-}\eta^2{:}\eta^2$ fashion, followed by electron transfer from the ferrous centers to the hydrazine resulting in N–N bond cleavage. A similar reaction leading to N–N bond cleavage and formation of a bridging imide could be envisioned in the FeMoco. Note that these cubane structures were obtained only with sterically hindered thiolates and 1,2-diarylhydrazines; all other substrates gave mixtures of products. In a different set of studies, iron-imide-sulfide heterocubanes were also structurally and spectroscopically characterized [118, 119].

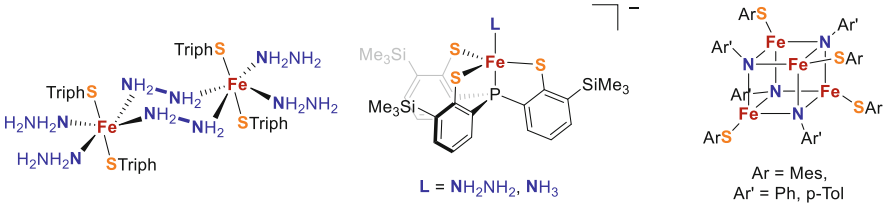

19 20 21

Fig. 9 Complexes generated by the addition of hydrazines to iron precursors with sterically bulky thiolate ligands

3.4 N_xH_y Complexes with Thiolate and Cp Ligands

Several complexes incorporating thiolate and Cp donors are also known to catalyze the N–N bond cleavage of hydrazines. Qu and coworkers reported that alkylthiolate-bridged iron complexes react with hydrazines to form *cis* diazene complexes (**22**) [120, 121]:

$$2\left[\mathrm{Cp^*Fe^{I}}\left(\mu\text{–}\mathrm{R^1SEt}\right)_3\mathrm{Fe^{II}Cp^*}\right] + 3\,\mathrm{R^2NH\text{–}NH_2} \rightarrow 2\left[\mathrm{Cp^*Fe^{II}}\left(\mu\text{–}\mathrm{R^1SEt}\right)_2\left(\mu\text{–}\mathrm{N_2R^2H}\right)\mathrm{Fe^{II}Cp^*}\right]\ (\mathbf{22}) + \mathrm{R^2NH_2} + \mathrm{NH_3} + 2\,\mathrm{HSR^1}$$

In the presence of reductant and acid, these compounds catalytically cleave the N–N bond of various alkyl- and aryl-substituted hydrazines. No intermediates could be detected in this reaction, but DFT calculations suggested that protonation and reduction of diazene involves isomerization to a (μ-NH)-NH_2 species [122]. The strong donation of the thiolates and their ability to shift coordination mode are thought to be important in allowing this isomerization to occur. Nishibayashi and coworkers reported a similar system containing an *ortho*-substituted aryl thiolate in which a methyldiazene (CH_3–N=NH) or methyldiazenido ($N{=}NCH_3^-$) moiety is bound side-on between two iron centers (**23**–**24**) [123] (Fig. 10). In this case, the bridging structure was important for promoting selective hydrazine cleavage; a corresponding monomeric complex promoted H_2 formation rather than NH_3 production. Again, however, the mechanism of N–N bond cleavage was not clear and the key hydrazido (R_2N-NR^-) intermediate could not be detected.

In another system, Qu and coworkers studied the generation of ammonia from treatment of a benzenedithiolate-bridged diiron complex with hydrazine [124]. Several intermediates along the pathway to NH_3 release were accessible via stepwise protonation and/or reduction. Starting from a diferrous complex with *cis*-diazene bound μ-η^1:η^1 between the iron centers (**25**), protonation led to electron transfer from the iron centers to the diazene ligand and rearrangement to afford a diferric complex in which a hydrazido ($N_2H_3^-$) ligand is bound asymmetrically in a μ-η^1:η^2 fashion (**26**). The bridging benzenedithiolate ligand also rearranged to a μ-η^1:η^2 coordination mode, which resembles the hypothesized rearrangement of sulfides in the FeMoco during turnover. Subsequent two-electron reduction and protonation of **26** resulted in ammonia release and formation of an amido-bridged diferrous complex (**27**). DFT calculations suggest that the ammonia comes from the non-bridging NH_2 of the hydrazido species via the mechanism shown in Fig. 11. Note that this process involves an NH–NH_3 intermediate that is not part of the traditional distal or alternating pathways but has been proposed for the FeMoco based on computational results [34]. The amido complex **27** also produces NH_3 upon further reduction and protonation, although the yield is low due to competitive proton reduction.

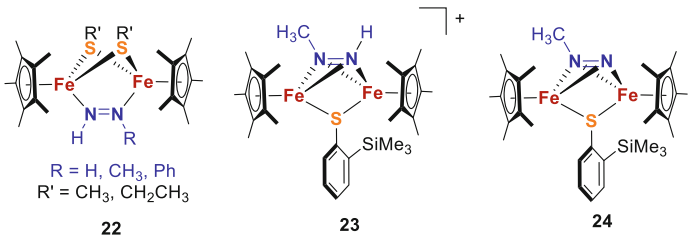

Fig. 10 Structures of Cp-supported thiolate-bridged diazene complexes reported by Qu and Nishibayashi

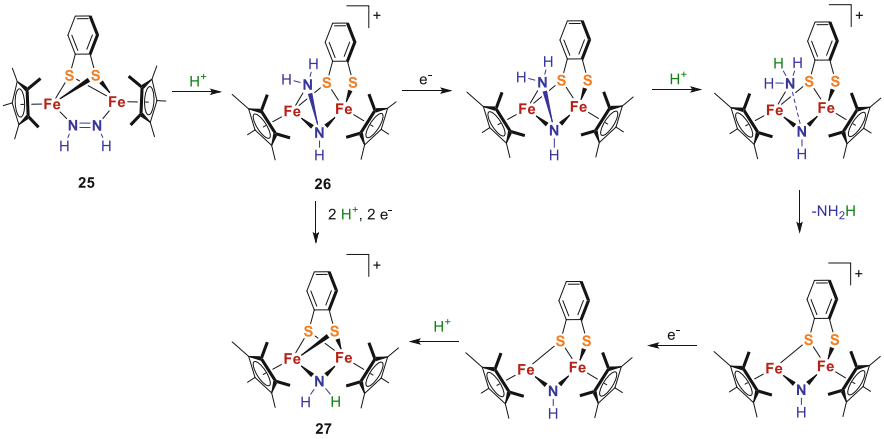

Fig. 11 Proposed mechanism of NH_3 release leading to the formation of **27** upon protonation and reduction of **25** via **26**. Of the complexes shown in this figure, only **26** and **27** are structurally characterized, although the structure of **25** (which is an isolable species) can be inferred based on the structure of the analogous one-electron oxidized species. The sequence of protonation and electron transfer steps is proposed based on DFT calculations

4 Conclusions

The results presented above show the variety of synthetic strategies that have yielded N_2 and N_xH_y complexes of iron with sulfur-containing supporting ligands. It is becoming clear that the coordinative flexibility, electron-rich character, and hydrogen-bonding capability of sulfur atoms can influence the behavior of bound N_2 and N_xH_y coligands. Understanding the electronic structure and reactivity of these compounds has begun to provide insight into the possible role(s) of the sulfides in the FeMoco of nitrogenase.

Acknowledgement The authors thank the National Institutes of Health (GM065313) for funding.

References

1. Ribbe M (ed) (2011) Nitrogen fixation. Humana, New York, NY
2. Burgess BK, Lowe DJ (1996) Chem Rev 96:2983
3. Holland PL (2004) Nitrogen fixation. In: McCleverty J, Meyer TJ (eds) Comprehensive Coordination Chemistry II. Elsevier, Oxford, Vol. 8, pp 569–599
4. Hu Y, Ribbe MW (2015) J Biol Inorg Chem 20:435
5. Hoffman BM, Lukoyanov D, Yang Z-Y, Dean DR, Seefeldt LC (2014) Chem Rev 114:4041
6. Eady RR (1996) Chem Rev 96:3013
7. Krahn E, Weiss BJR, Kröckel M, Groppe J, Henkel G, Cramer SP, Trautwein AX, Schneider K, Müller A (2002) J Biol Inorg Chem 7:37
8. Seefeldt LC, Dance IG, Dean DR (2004) Biochemistry 43:1401
9. Spatzal T, Schlesier J, Burger E-M, Sippel D, Zhang L, Andrade SLA, Rees DC, Einsle O (2016) Nat Commun 7:10902
10. Bjornsson R, Lima FA, Spatzal T, Weyhermüller T, Glatzel P, Bill E, Einsle O, Neese F, DeBeer S (2014) Chem Sci 5:3096
11. Hoffman BM, Dean DR, Seefeldt LC (2009) Acc Chem Res 42:609
12. Seefeldt LC, Hoffman BM, Dean DR (2009) Annu Rev Biochem 78:701
13. Hoffman BM, Lukoyanov D, Dean DR, Seefeldt LC (2013) Acc Chem Res 46:587
14. Lukoyanov D, Yang Z-Y, Khadka N, Dean DR, Seefeldt LC, Hoffman BM (2015) J Am Chem Soc 137:3610
15. Thorneley RNF, Lowe DJ (1985) Met Ions Biol 7:221
16. Igarashi RY, Laryukhin M, Dos Santos PC, Lee H-I, Dean DR, Seefeldt LC, Hoffman BM (2005) J Am Chem Soc 127:6231
17. Lukoyanov D, Yang Z-Y, Dean DR, Seefeldt LC, Hoffman BM (2010) J Am Chem Soc 132:2526
18. Doan PE, Telser J, Barney BM, Igarashi RY, Dean DR, Seefeldt LC, Hoffman BM (2011) J Am Chem Soc 133:17329
19. Schrock RR (2005) Acc Chem Res 38:955
20. Nishibayashi Y (2015) Inorg Chem 54:9234
21. Rittle J, Peters JC (2016) J Am Chem Soc 138:4243
22. Lee SC, Holm RH (2003) Proc Natl Acad Sci U S A 100:3595
23. Lee SC, Holm RH (2004) Chem Rev 104:1135
24. Lee SC, Lo W, Holm RH (2014) Chem Rev 114:3579
25. Spatzal T, Perez KA, Einsle O, Howard JB, Rees DC (2014) Science 345:1620
26. Spatzal T, Perez KA, Howard JB, Rees DC (2015) Elife 4:e11620
27. Wiig JA, Lee CC, Hu Y, Ribbe MW (2013) J Am Chem Soc 135:4982
28. Dance I (2008) Dalton Trans 5977
29. Dance I (2008) Dalton Trans 5992
30. Dance I (2012) Dalton Trans 41:4859
31. Dance I (2014) A unified chemical mechanism for hydrogenation reactions catalyzed by nitrogenase. In: Weigand W, Schollhammer P (eds) Bioinspired catalysis. Wiley, Weinheim, pp 249–288
32. Huniar U, Ahlrichs R, Coucouvanis D (2004) J Am Chem Soc 126:2588
33. Schimpl J, Petrilli HM, Blöchl PE (2003) J Am Chem Soc 125:15772
34. Kästner J, Blöchl PE (2007) J Am Chem Soc 129:2998
35. Hinnemann B, Nørskov JK (2004) J Am Chem Soc 126:3920
36. Varley JB, Wang Y, Chan K, Studt F, Nørskov JK (2015) Phys Chem Chem Phys 17:29541
37. Rao L, Xu X, Adamo C (2016) ACS Catalysis 6:1567
38. McKee ML (2016) J Phys Chem A 120:754
39. Siegbahn PEM (2016) J Am Chem Soc 138:10485
40. Rodriguez MM, Bill E, Brennessel WW, Holland PL (2011) Science 334:780
41. Grubel K, Brennessel WW, Mercado BQ, Holland PL (2014) J Am Chem Soc 136:16807

42. MacLeod KC, McWilliams SF, Mercado BQ, Holland PL (2016) Chem Sci 7:5736
43. Lee Y, Sloane FT, Blondin G, Abboud KA, García-Serres R, Murray LJ (2015) Angew Chem Int Ed Engl 54:1499
44. Anderson JS, Rittle J, Peters JC (2013) Nature 501:84
45. Creutz SE, Peters JC (2014) J Am Chem Soc 136:1105
46. Ung G, Peters JC (2015) Angew Chem Int Ed Engl 54:532
47. Del Castillo TJ, Thompson NB, Peters JC (2016) J Am Chem Soc 138:5341
48. Yuki M, Tanaka H, Sasaki K, Miyake Y, Yoshizawa K, Nishibayashi Y (2012) Nat Commun 3:1254
49. Kuriyama S, Arashiba K, Nakajima K, Matsuo Y, Tanaka H, Ishii K, Yoshizawa K, Nishibayashi Y (2016) Nat Commun 7:12181
50. MacKay BA, Fryzuk MD (2004) Chem Rev 104:385
51. Crossland JL, Tyler DR (2010) Coord Chem Rev 254:1883
52. Hazari N (2010) Chem Soc Rev 39:4044
53. MacLeod KC, Holland PL (2013) Nat Chem 5:559
54. Köthe C, Limberg C (2015) Z Anorg Allg Chem 641:18
55. Tanabe Y, Nishibayashi Y (2016) Chem Rec 16:1549
56. Ohki Y, Seino H (2016) Dalton Trans 45:874
57. Čorić I, Holland PL (2016) J Am Chem Soc 138:7200
58. Hallmen PP, Kästner J (2015) Z Anorg Allg Chem 641:118
59. Bazhenova TA, Shilov AE (1995) Coord Chem Rev 144:69
60. NIST Computational Chemistry Comparison and Benchmark Database (2015) National Institute of Standards and Technology. http://cccbdb.nist.gov/. Accessed 21 Sept 2015
61. Bart SC, Lobkovsky E, Bill E, Wieghardt K, Chirik PJ (2007) Inorg Chem 46:7055
62. Lee Y, Mankad NP, Peters JC (2010) Nat Chem 2:558
63. Takaoka A, Mankad NP, Peters JC (2011) J Am Chem Soc 133:8440
64. Creutz SE, Peters JC (2015) J Am Chem Soc 137:7310
65. Čorić I, Mercado BQ, Bill E, Vinyard DJ, Holland PL (2015) Nature 526:96
66. McWilliams SF, Holland PL (2015) Acc Chem Res 48:2059
67. Venkateswara Rao P, Holm RH (2004) Chem Rev 104:527
68. Henderson RA (2014) Binding substrates to synthetic Fe–S-based clusters and the possible relevance to nitrogenases. In: Weigand W, Schollhammer P (eds) Bioinspired catalysis. Wiley, Weinheim, pp 289–324
69. Tanaka K, Hozumi Y, Tanaka T (1982) Chem Lett 11:1203
70. Banerjee A, Yuhas BD, Margulies EA, Zhang Y, Shim Y, Wasielewski MR, Kanatzidis MG (2015) J Am Chem Soc 137:2030
71. Liu J, Kelley MS, Wu W, Banerjee A, Douvalis AP, Wu J, Zhang Y, Schatz GC, Kanatzidis MG (2016) Proc Natl Acad Sci U S A 113:5530
72. Heim HC, Bernhardt TM, Lang SM, Barnett RN, Landman U (2016) J Phys Chem C 120:12549
73. Arnet NA, Dugan TR, Menges FS, Mercado BQ, Brennessel WW, Bill E, Johnson MA, Holland PL (2015) J Am Chem Soc 137:13220
74. Yang Z-Y, Khadka N, Lukoyanov D, Hoffman BM, Dean DR, Seefeldt LC (2013) Proc Natl Acad Sci U S A 110:16327
75. Lukoyanov D, Khadka N, Yang Z-Y, Dean DR, Seefeldt LC, Hoffman BM (2016) J Am Chem Soc 138:10674
76. Lukoyanov D, Khadka N, Yang Z-Y, Dean DR, Seefeldt LC, Hoffman BM (2016) J Am Chem Soc 138:1320
77. Stanbury DM (1991) Inorg Chem 30:1293
78. Liao G-L, Palmer G (1998) Biochemistry 37:15583
79. Barney BM, McClead J, Lukoyanov D, Laryukhin M, Yang T-C, Dean DR, Hoffman BM, Seefeldt LC (2007) Biochemistry 46:6784
80. Hozumi Y, Imasaka Y, Tanaka K, Tanaka T (1983) Chem Lett 12:897

81. Coucouvanis D, Mosier PE, Demadis KD, Patton S, Malinak SM, Kim CG, Tyson MA (1993) J Am Chem Soc 115:12193
82. Malinak SM, Demadis KD, Coucouvanis D (1995) J Am Chem Soc 117:3126
83. Demadis KD, Malinak SM, Coucouvanis D (1996) Inorg Chem 35:4038
84. Malinak SM, Simeonov AM, Mosier PE, McKenna CE, Coucouvanis D (1997) J Am Chem Soc 119:1662
85. Palermo RE, Singh R, Bashkin JK, Holm RH (1984) J Am Chem Soc 106:2600
86. Coucouvanis D (1996) J Biol Inorg Chem 1:594
87. Demadis KD, Coucouvanis D (1994) Inorg Chem 33:4195
88. Demadis KD, Coucouvanis D (1995) Inorg Chem 34:3658
89. Coucouvanis D, Demadis KD, Malinak SM, Mosier PE, Tyson MA, Laughlin LJ (1996) J Mol Catal A Chem 107:123
90. Vela J, Stoian S, Flaschenriem CJ, Münck E, Holland PL (2004) J Am Chem Soc 126:4522
91. Stubbert BD, Vela J, Brennessel WW, Holland PL (2013) Z Anorg Allg Chem 639:1351
92. Lees NS, McNaughton RL, Vargas Gregory W, Holland PL, Hoffman BM (2008) J Am Chem Soc 130:546
93. Sellmann D, Sutter J (1997) Acc Chem Res 30:460
94. Sellmann D, Utz J, Blum N, Heinemann FW (1999) Coord Chem Rev 190–192:607
95. Sellmann D, Sutter J (1996) J Biol Inorg Chem 1:587
96. Sellmann D, Soglowek W, Knoch F, Moll M (1989) Angew Chem Int Ed Engl 28:1271
97. Sellmann D, Friedrich H, Knoch F, Moll M (1994) Z Naturforsch B 49:76
98. Sellmann D, Hennige A (1997) Angew Chem Int Ed Engl 36:276
99. Sellmann D, Blum DCF, Heinemann FW (2002) Inorg Chim Acta 337:1
100. Reiher M, Sellmann D, Hess AB (2001) Theor Chem Acc 106:379
101. Reiher M, Salomon O, Sellmann D, Hess BA (2001) Chem Eur J 7:5195
102. Lehnert N, Wiesler BE, Tuczek F, Hennige A, Sellmann D (1997) J Am Chem Soc 119:8869
103. Lehnert N, Wiesler BE, Tuczek F, Hennige A, Sellmann D (1997) J Am Chem Soc 119:8879
104. Carlotti M, Johns JWC, Trombetti A (1974) Can J Phys 52:340
105. Bondybey VE, Nibler JW (1973) J Chem Phys 58:2125
106. Giguère PA, Liu ID (1952) J Chem Phys 20:136
107. Sellmann D, Soglowek W, Knoch F, Ritter G, Dengler J (1992) Inorg Chem 31:3711
108. Sellmann D, Shaban S, Heinemann F (2004) Eur J Inorg Chem 2004:4591
109. Sellmann D, Blum N, Heinemann F (2001) Z Naturforsch B 56:581
110. Sellmann D, Hennige A, Heinemann FW (1998) Inorg Chim Acta 280:39
111. Sellmann D, Hofmann T, Knoch F (1994) Inorg Chim Acta 224:61
112. Sellmann D, Kreutzer P, Huttner G, Frank A (1978) Z Naturforsch B 33:1341
113. Sellmann D, Friedrich H, Knoch F (1994) Z Naturforsch B 49:660
114. Zdilla MJ, Verma AK, Lee SC (2008) Inorg Chem 47:11382
115. Chang Y-H, Chan P-M, Tsai Y-F, Lee G-H, Hsu H-F (2014) Inorg Chem 53:664
116. Verma AK, Lee SC (1999) J Am Chem Soc 121:10838
117. Zdilla MJ, Verma AK, Lee SC (2011) Inorg Chem 50:1551
118. Chen X-D, Duncan JS, Verma AK, Lee SC (2010) J Am Chem Soc 132:15884
119. Chen X-D, Zhang W, Duncan JS, Lee SC (2012) Inorg Chem 51:12891
120. Chen Y, Zhou Y, Chen P, Tao Y, Li Y, Qu J (2008) J Am Chem Soc 130:15250
121. Chen Y, Liu L, Peng Y, Chen P, Luo Y, Qu J (2011) J Am Chem Soc 133:1147
122. Luo Y, Li Y, Yu H, Zhao J, Chen Y, Hou Z, Qu J (2012) Organometallics 31:335
123. Yuki M, Miyake Y, Nishibayashi Y (2012) Organometallics 31:2953
124. Li Y, Li Y, Wang B, Luo Y, Yang D, Tong P, Zhao J, Luo L, Zhou Y, Chen S, Cheng F, Qu J (2013) Nat Chem 5:320